Titration of the Phase Transition of Phosphatidylserine Bilayer Membranes. Effects of pH, Surface Electrostatics, Ion Binding, and Head-Group Hydration†

Gregor Cevc,*‡ Anthony Watts, and Derek Marsh*

ABSTRACT: The dependence of the gel-to-fluid phase transition temperature of dimyristoyl- and dipalmitoylphosphatidylserine bilayers on pH, NaCl concentration, and degree of hydration has been studied with differential scanning calorimetry and with spin-labels. On protonation of the carboxyl group (pK_2^{app} = 5.5), the transition temperature increases from 36 to 44 °C in the fully hydrated state of dimyristoylphosphatidylserine (from 54 to 62 °C for dipalmitoylphosphatidylserine), at ionic strength J = 0.1. In addition, at least two less hydrated states, differing progressively by 1 H_2O/PS, are observed at low pH with transition temperatures of 48 and 52 °C for dimyristoyl- and 65 and 68.5 °C for dipalmitoylphosphatidylserine. On deprotonation of the amino group (pK_3^{app} = 11.55) the transition temperature decreases to ~15 °C for dimyristoyl- and 32 °C for dipalmitoylphosphatidylserine, and a pretransition is observed at ~6 °C (dimyristoylphosphatidylserine) and 21.5 °C (dipalmitoylphosphatidylserine), at J = 0.1. No titration of the transition is observed for the fully hydrated phosphate group down to pH ≥0.5, but its affinity for water binding decreases steeply at pH ≤2.6. Increasing the NaCl concentration from 0.1 to 2.0 M increases the transition temperature of dimyristoylphosphatidylserine by ~8 °C at pH 7, by ~5 °C at pH 13, and by ~0 °C at pH 1. These increases are attributed to the screening of the electrostatic titration-induced shifts in transition temperature. On a further increase of the NaCl concentration to 5.5 M, the transition temperature increases by an additional 9 °C at pH 7, 13 °C at pH 13, ~7 °C in the fully hydrated state at pH 1, and ~4 and ~0 °C in the two less hydrated states. These shifts are attributed to displacement of water of hydration by ion binding. From the salt dependence it is deduced that the transition temperature shift at the carboxyl titration can be accounted for completely by the surface charge and change in hydration of ~1 H_2O/lipid, whereas that of the amino group titration arises mostly from other sources, probably hydrogen bonding. The shifts in pK (ΔpK_2 = 2.85, ΔpK_3 = 1.56) are consistent with a reduced polarity in the head-group region, corresponding to an effective dielectric constant $\epsilon \simeq 30$, together with surface potentials of $\psi \simeq -100$ and −150 mV at the carboxyl and amino group pKs, respectively. The transition temperature of dimyristoylphosphatidylserine–water mixtures decreases by ~4 °C for each water/lipid molecule added, reaching a limiting value at a water content of ~9–10 H_2O/lipid molecule.

Phosphatidylserine is the major negatively charged phospholipid of mammallian cell membranes (White, 1973). Its anionic character at physiological pH makes this lipid especially important in processes involving the interactions between the membrane and the intra- and extracellular electrolytes. Both the ion-binding and ion-exchange properties provide potential means of membrane signal transduction, via changes in the external ionic concentrations. Phosphatidylserine may also play an important role in the interactions between cell membranes (Nir & Bentz, 1978; Papahadjopoulos, 1978).

Bilayer membranes composed of phospholipids with uniform, defined fatty acid chain composition undergo a characteristic order–disorder phase transition in the hydrocarbon chain region, which has been of considerable utility in studying biomembrane structure (Träuble, 1971, 1976; Melchior & Steim, 1976). The phase transition temperatures of all negatively charged lipid bilayers have been shown to depend sensitively on the ionic composition of the aqueous medium: on the concentration of protons and other monovalent, as well as divalent, cations. (Verkleij et al., 1974; Träuble & Eibl, 1974; Jacobson & Papahadjopoulos, 1975; Watts et al., 1978).

In the present work we have studied the titration of the phase transition temperature of dimyristoyl- and dipalmitoylphosphatidylserine multibilayers in the range of pH ~0.5–14 and also its dependence on the degree of lipid hydration and sodium ion concentration. This work differs from previous studies (MacDonald et al., 1976; van Dijck et al., 1978) in the increased pH range, the characterization of the hydration effects, and the more detailed attention paid to the salt effects. Two titration regions of the transition temperature, with apparent p$K \simeq 5.5$, corresponding to the carboxyl group, and with apparent p$K \simeq 11.5$, corresponding to the ammonium group (both at ionic strength 0.1) of the serine segment, were determined. The latter was not observed in previous work, and also the pretransition which appears after the deprotonation of the ammonium group of the phosphatidylserine is reported for the first time. When the carboxyl group is protonated, the lipid does not hydrate readily, and the transition temperatures determined in this work are the first for maximally hydrated phosphatidylserine bilayers in the zwitterionic state, i.e., with protonated carboxyl group. The dependence of the transition temperature on salt concentration defines the electrostatic contribution to the pH-induced phase transition temperature shift and is also indicative of sodium ion binding to the phosphatidylserine head group at a site which is involved in water binding. It is found that the contribution of the carboxyl group titration to the phase transition can be accounted for in terms of the changes in head-group hydration and surface electrostatics; the ammonium group titration, however, has a predominantly nonelectrostatic origin in the fully hydrated state. This nonelectrostatic contribution probably originates in the changes in intermolecular hydrogen bonding, in the tilt of the acyl chains, and possibly other

† From the Max-Planck-Institut für biophysikalische Chemie, Abteilung Spektroskopie, D-3400 Göttingen, Federal Republic of Germany. *Received January 30, 1981.* This work was supported in part by the Deutsche Forschungsgemeinschaft (Grant No. Ma 756/1 to D.M.). G.C. received a fellowship from the Deutscher Akademischer Austauschdienst.

‡ Permanent address: Institute for Biophysics and Institute J. Stefan, University E. Kardelj, 6100 Ljubljana, Yugoslavia.

0006-2960/81/0420-4955$01.25/0

conformation changes. This study of the lipid phase transition thus elucidates a major part of the phase diagram of phosphatidylserine bilayers and gives some appreciation of the range of possible ionic interactions involving the head group of this lipid.

Materials and Methods

Lipids. 1,2-Dimyristoyl-*sn*-glycero-3-phosphoethanolamine (DMPE)[1] and 1,2-diacyl-*sn*-glycero-3-phosphocholines were purchased from Fluka (Buchs, Switzerland); they were shown to be pure by thin-layer chromatography on silicic acid plates and were used without further purification.

1,2-Diacyl-*sn*-glycero-3-phospho-L-serine was prepared by enzymatic transphosphatidylation with phospholipase D (Boehringer, Mannheim, Federal Republic of Germany) from the corresponding phosphocholine in the presence of excess L-serine (Fluka, Buchs, Switzerland) following the procedure and purification method of Comfurius & Zwaal (1977) which includes washing with EDTA. The chromatographed lipid was crystallized from acetone as the free acid. The sodium salt was prepared by shaking the lipid in chloroform/methanol/sodium borate buffer (pH 9), and the concentrated lipid was again crystallized from acetone. Vacuum dried lipid (0.01 Torr, >24 h) was stored at −20 °C until needed. Purified phosphatidylserine cochromatographed as a single spot on silicic acid TLC plates with bovine brain phosphatidylserine of Lipid Products (Surrey, England) by using the solvent system $CH_3Cl/CH_3OH/30\%\ NH_4OH$ (10:10:3 v/v/v), when detected with ninhydrin and molybdenum blue sprays, followed by charring. Anal. Calcd for $C_{34}H_{66}N_{10}P\cdot H_2O$: C, 58.6; H, 9.75; N, 2.01; P, 4.45. Anal. Found: C, 58.4; H, 9.36; N, 2.09; P, 4.38.

Other Chemicals. Solvents were P.A. grade and salts were of Merck (Darmstadt, FRG) Suprapur grade although the use of P. A. salts yielded the same results. All buffers contained 10 μmol L^{-1} of EDTA and were prepared with doubly distilled water (increasing the EDTA concentration to 50 μM had no effect on the results); final ionic strength was adjusted by addition of the appropriate amounts of sodium chloride and was, unless stated otherwise, 0.1. When possible, two buffer types were used in the pH regions of limiting buffering capacity. The spin-label Tempo was prepared according to the method of Rosantzev & Neiman (1964), and the C-11 spin-label was prepared by Dr. W. Kühnle of this institute.

Lipid dispersions for the ESR experiments were always prepared from finely powdered, dry lipid; depending on the desired pH, several procedures for preparing lipid dispersions were employed.

(1) For experiments performed at $4.5 \leq pH \leq 10$, dry phosphatidylserine was dispersed in buffer at ~40 °C by vortex mixing to give a uniformly opaque dispersion to which spin-label in water solution was added. Typical lipid concentrations were 2.5 and 25 mM with spin-label concentrations of 25 μM and 0.125 mM for C-11 and Tempo experiments, respectively. The pH of the dispersions was determined by a pH meter at 22 °C to within 0.05 unit and was found constant after a set of experiments. The lipid purity after an experiment was frequently checked by TLC.

(2) At $3 \leq pH \leq 4.5$, the lipid hydrated less readily even when it was heated to $T \geq T_t$ for a short time. Therefore, the lipid was mixed with buffer at $T \leq T_t$ by vigorous vortex mixing, and spin-label was added. The mixture was centrifuged (2000*g*, 3 min) in the measuring glass capillary. Hydration was performed in the first heating scan in the spectrometer.

(3) At pH ≤3, the lipid–buffer mixtures were prepared as for (2), but the lipid concentration (as free acid) was increased to 5 mM and the spin-label/lipid ratio was increased to 3–5% because of the strong free radical reduction, which also made multiple scans using Tempo irreproducible. Even after prolonged vortex mixing at $T > T_t$ such samples still retained clearly visible crystalline structure typical of unhydrated lipid. The pellet was put into the capillary tubes and used for experiments. The pH of such dispersions did not differ significantly before and after the temperature runs. Since the results of the first and the subsequent temperature scans to $T \gg T_t$ using the samples prepared in this manner differed considerably, the origin of the difference was elucidated by making the PS dispersions of pH ≲3 also in other ways, as follows. (a) The samples without spin-label, prepared as described above, were incubated at 90 °C for 1 min, in which time most of the lipid settled out. The sample was cooled to room temperature, spin-labeled before it was centrifuged, and further used for measurements as in (2). (b) The time of incubation at 90 °C was prolonged to 15–18 min with intermittent vortex mixing since it was found that this incubation time sufficed for full hydration of the lipid. Then, the samples were treated as in (2). (c) Dry, powdered lipid was mixed with typically 10 μL of the spin-label solution in water, briefly heated to 40 °C > T_t, and mixed until the dispersion was homogeneous. (In our experience, different batches of lipid, although equally pure chromatographically and in the same ionization state, exhibit different affinities for water. The reasons for this may be due to the different crystalline states of dry lipid and/or the number of crystalline water molecules [see also Browning & Seelig (1979)].) Then, 0.3 mL of appropriate buffer was added to the dispersion and the mixture vortex mixed until it again became homogeneous. Such samples were as a rule stable and did not degrade even at pH ≃1 and after several temperature scans (to T_t + 10 °C).

(4) Experiments in the alkaline region, pH >10 were performed with the lipid dispersions which were prepared similarly to (1), the main difference being that the lipid concentration was 1 mM and that the spin-label/lipid concentration was increased to 7.5–10%. Also, the dispersions of PS at pH ≳12.5 were made at 4 °C, and only the first two temperature scans were considered.

All the samples were routinely checked by TLC run in $CHCl_3/CH_3OH/NH_4OH$ (10:10:3 v/v/v) after the temperature scans. The results of the experiments which showed more than 5% degradation were rejected and the measurements repeated. In strongly alkaline buffers the hydrolysis of the lipid occurred fast due to the instability of the ester bond: at pH ~13 and at $T \gg T_t$, the half-time of lipid degradation was ~15 min. At $T < T_t$, however, the rate of deterioration was slower.

Determination of the Phase Transition Temperatures. (*1*) *ESR measurements* were made with a Varian E-12 9-GHz ESR spectrometer. The lipid dispersions, contained in sealed-off, 100-μL glass capillary tubes, were put into a 4-mm standard quartz tube filled with silicon oil to ensure that the

[1] Abbreviations used: DMPS, 1,2-dimyristoyl-*sn*-glycero-3-phospho-L-serine; DPPS, 1,2-dipalmitoyl-*sn*-glycero-3-phospho-L-serine; DMPE, 1,2-dimyristoyl-*sn*-glycero-3-phosphoethanolamine; BBPS, bovine brain phosphatidylserine; C-11 spin-label, 2,2-di(1-pentyl)-4,4′-dimethyl-3-oxazolidinyloxy; Tempo, 2,2,6,6-tetramethylpiperidinyl-*N*-oxy; DSC, differential scanning calorimetry; TLC, thin-layer chromatography; ESR, electron spin resonance; PS, 1,2-diacylglycero-3-phospho-L-serine; T_p, pretransition temperature; T_t, main gel–fluid phase transition temperature; EDTA, ethylenediaminetetraacetic acid; Pipes, 1,4-piperazinediethanesulfonic acid.

Table I: Phase Transition Temperatures (°C), Enthalpies [kJ mol^{-1} (kcal mol^{-1})], and Entropies [J mol^{-1} K^{-1} (cal mol^{-1} K^{-1})] of PS Bilayers[a]

	pH 1[e]		pH 7			pH 13		
	DMPS	DPPS		DMPS	DPPS		DMPS	DPPS
DSC								
T_{1t}	44[b]	62[b]						
T_{2t}	48	65	T_t^-	36	54	T_t^{2-}	[15][d]	32
T_{3t}	52	68.5		43.5[c]				38[c]
ΔH_{1t}	27.3 (6.5)[b]	36.1 (8.6)[b]						
ΔH_{2t}	25.2 (6.0)	35.3 (8.5)	ΔH_t^-	29 (6.9)	37.4 (8.9)	ΔH_t^{2-}	[25 (6.0)]	33.6 (8.0)
ΔH_{3t}	22.3 (5.3)			29.4 (7)[c]				
ΔS_{1t}	86.5 (20.5)	104 (24.8)	ΔS_t^-	94 (22.3)	115 (27.3)	ΔH_t^{2-}	[87.5 (20.8)]	110 (26.2)
ESR (Tempo)			T_t^-	35	53			
ESR (C-11)								
T_{1t}	39	58						
T_{2t}	43	61	T_t^-	31	48	T_t^{2-}	7	25
T_{3t}	47	63						
T_p (ESR)							1.5	18.5
T_p (DSC)							[6]	21.5
								28[c]
ΔH_p								5.5 (1.3)

[a] $J = 0.1$, 10 μM EDTA; each value is the average of at least four independent measurements. [b] No salt, 3 M PS·H, in doubly distilled water. [c] $J = 1.0$. [d] DSC values for DMPS at pH 13 in brackets correspond to samples for which there was detectable chemical degradation. [e] For definition of T_{1t}, T_{2t}, and T_{3t}, see text.

temperature gradients within the sample tubes were <1 °C cm^{-1}. The temperature within the measuring Dewar insert was controlled by a heated–cooled stream of N_2 gas. Transition temperatures were then measured and determined by continuously monitoring the ESR line heights of the spin-label partitioned in the lipid ($0.5 \leq$ pH $\lesssim 10$) or water (pH > 10) medium. Typical temperature scanning rates were 2.5 or 5 °C min^{-1}. The spectrometer was locked to the monitored peak, and the microwave detector bias current was kept constant by an automatic coupling iris adjustment [see Watts et al. (1978)]. By locking onto the ESR peak, shifts in line position (due both to changes in cavity frequency and to intrinsic spectral changes) are automatically compensated. Continuous monitoring of the ESR line height gave results identical with those obtained from point-by-point measurement of the changes in spin-label partitioning through the transition [for further details see Marsh & Watts (1981)]. Typical reproducibility of transition temperature measurement was ±0.5 °C.

(2) *Differential scanning calorimetry measurements* were made with a Perkin-Elmer DSC-2 calorimeter. Typically, ~2.5 mg of dry lipid and 50 μL of the appropriate buffer were put into the measuring pan (large volume), sealed off, and immediately used for experiment. The reference pan always contained 50 μL of the corresponding buffer. For the T_t determinations at low pH, the free acid form of the lipid was employed, while in experiments at pH >7 the dispersions were made with the sodium salt.

For the studies of lipid hydration, finelly pulverized, dry lipid was kept for >48 h under vacuum (0.01 Torr) in presence of P_2O_5. The lipid was then sealed in plastic ampules, and a freshly opened ampule was used for each experiment. The lipid was weighed into the pan and covered with parafilm. A water droplet was put in the top part of the pan and its mass monitored for 3 min. After the pan was sealed, the corrections were made for the evaporation losses which occurred during the sample manipulation, on the basis of the evaporation rate determined previously. The accurate molar lipid/water ratio could then be calculated. Hydration of the samples under an atmosphere of defined humidity using saturated salt solutions (the lipid/water ratio was again determined gravimetrically) yielded essentially the same results.

The heating rates were 2.5 or 5 °C min^{-1}. Heat flow was 0.48 mJ s^{-1} (2 mcal s^{-1}). At least two cycles were made with each sample, and, unless stated otherwise, the average values of T_t and ΔH_t were used in analysis of the results. Transition enthalpies were determined by measuring the area under the excess heat vs. temperature curves by paper weighing. The molar values were then calculated from the known amount of the lipid used for the experiment.

Results

The phase transition behavior of dimyristoyl- and dipalmitoylphosphatidylserine has been investigated by differential scanning calorimetry and by spin-label partitioning. Spin-label ESR was used to determine the titration behavior and salt dependence of the transition temperature because considerably lower lipid concentrations were needed than for DSC. This made it much easier to prepare dispersions of defined pH and salt concentration, especially at extreme pH values, at which lipid degradation had to be contended with.

Differential Scanning Calorimetry: T_t, ΔH_t, and ΔS_t. The transition temperatures, enthalpies and entropies of DMPS and DPPS multibilayer dispersions are given in Table I. They were determined at pH 1, pH 7, and pH 13, corresponding to the zwitterionic, singly negatively charged, and doubly negatively charged states of PS (see below). Representative DSC scans for DPPS are given in Figure 1. Notable is the occurrence of a pretransition, of smaller enthalpy than the main transition, at pH ~13. The lipid was subject to chemical degradation at pH >12 when above the phase transition. Thus, although completely reproduceable results were obtained for DPPS on the first upward scans, the data for DMPS were less so since the phase transition of the latter is below room temperature. For this reason, the DSC data for DMPS at pH 13 in Table I must be considered as only approximate.

At pH 1, PS hydrates less readily than at the higher pH values. Three different states with transition temperatures T_{3t}, T_{2t}, and T_{1t} are observed depending on the method of preparation and sample history. The states are defined by the

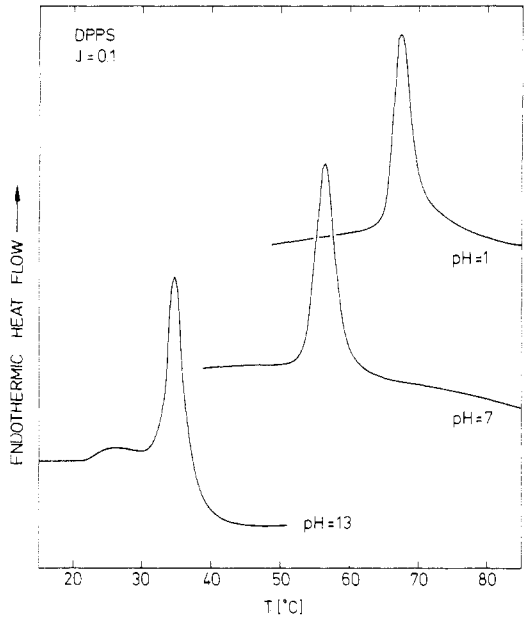

FIGURE 1: Differential scanning calorimetry recordings of DPPS dispersions as a function of the bulk pH. (pH 1) The second heating run of a free acid sample dispersed in 0.1 N HCl, which was heated once to 100 °C and then cooled to 0 °C; (pH 7) typical heating scan in neutral pH buffer; (pH 13) first heating run in 0.1 N NaOH. All buffers contained 10 μM EDTA, and the scanning rates were 5 °C min^{-1}.

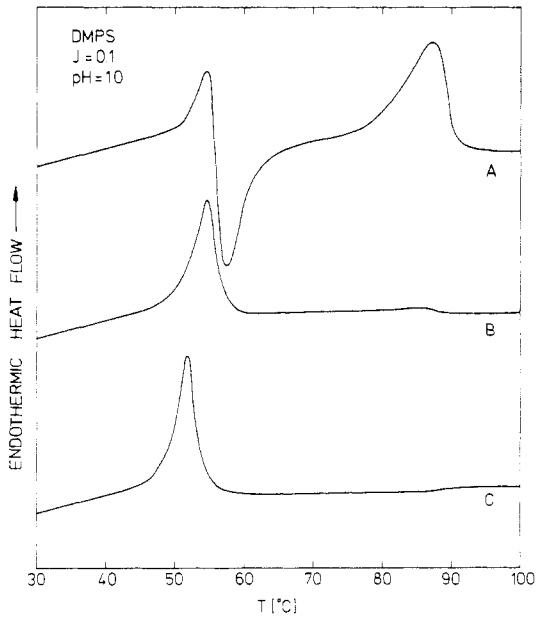

FIGURE 2: Differential scanning calorigrams of DMPS (free acid) in 0.1 N HCl and 10 μM EDTA, as a function of pretreatment of the sample. (a) First heating scan from 0 to 100 °C; (b) reheating after one heating run, 0–100 °C, following by immediate cooling to 0 °C; (c) heating scan made after incubation of the sample at 90 °C (30 min) and cooling to 0 °C. The heating and cooling rates were 5 °C min^{-1}.

preparation method, and it is argued below that they correspond to increasing degrees of hydration. A typical sequence of DSC scans for DMPS samples with progressively increasing degrees of hydration is given in Figure 2. On the first heating run (Figure 2A) a small endothermic peak at $T_{3t} \simeq 52$ °C ($T_{3t} \simeq 68.5$ °C for DPPS) is followed immediately by an exothermic transition of varying enthalpy ($\sim$1.5 × that of the endothermic transition), and a broad endothermic peak, which does not occur on subsequent runs, is observed at 84 ± 2.5 °C (89.5 ± 2.5 °C for DPPS). This latter transition corresponds

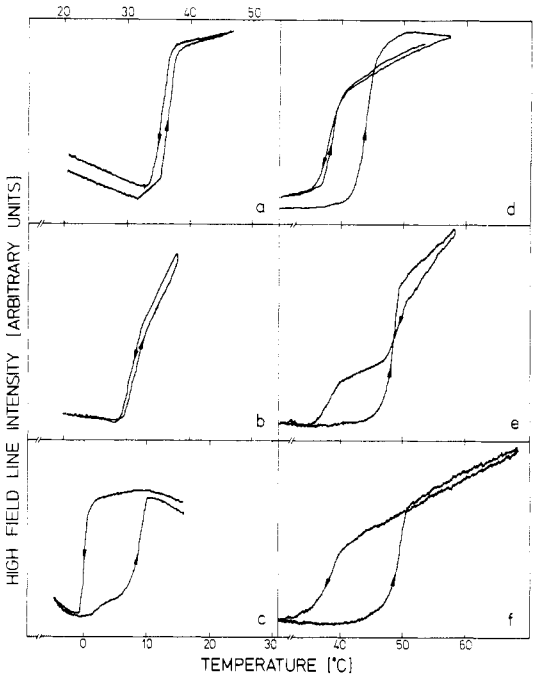

FIGURE 3: Temperature dependence of high-field ESR line height of partitioning spin-labels in DMPS dispersions. The lipid phase line height was monitored for the C-11 label at pH $\lesssim$9, and the aqueous (negative) line height was monitored for the Tempo label and for the C-11 label at pH $\gtrsim$9. (a) Tempo (10^{-4} M) in 25 mM DMPS dispersion, pH 7.0; (b) C-11 label (25 μM) in 2.5 mM DMPS, pH 7.0; (c) C-11 label (75 μM) in 1.25 mM DMPS, pH 12.5; (d) C-11 label (50 μM) in 2.5 mM DMPS, pH 3.5; (e) C-11 label (125 μM) in 2.5 mM DMPS, pH 2.6; (f) as in (e), except with heating to high $T \gg T_t$ during the temperature cycle. Scan rate, 2.5 °C min^{-1}; buffer ionic strength, 0.1, with 10 μM EDTA in all cases.

closely in temperature to the transition of the anhydrous lipid we observe by DSC and is presumably associated with the unhydrated lipid. On the second and subsequent scans (Figure 2B) which immediately followed the first one, all of the calorimetric enthalpy ($\Delta H_{3t} \simeq 22$ kJ/mol) was observed in the 52 °C transition. Storing the DSC sample of DMPS above the anhydrous transition temperature for prolonged periods of time (15–45 min) resulted in a downward shift of the transition to a temperature centered around $T_{2t} \simeq 48$ °C with $\Delta H_{2t} \simeq 25$ kJ/mol (see Figure 2C). TLC analysis failed to indicate notable lipid degradation following this high-temperature incubation. A similar state was achieved in DPPS simply on the first normal cooling cycle and all subsequent runs: $T_{2t} \simeq 65$ °C with $\Delta H_{2t} \simeq 35$ kJ/mol (8.5 kcal/mol) was determined. A third state of even greater hydration was obtained when the free acid form of the lipid was mixed with small volumes of water (for which the buffering capacity of the lipid sufficed to keep the carboxyl group in the protonated state). In the range of lipid concentrations 2–6 M, the transition temperature was then centered at $T_{1t} \simeq 44$ °C for DMPS with a transition enthalpy $\Delta H_{1t} \simeq 27$ kJ/mol ($T_{1t} \simeq 63$ °C, $\Delta H_{1t} \simeq 26.1$ kJ/mol for DPPS).

Spin-Label Transition Temperatures. A typical transition curve obtained from the partitioning of the Tempo spin-label is given in Figure 3a. The Tempo-derived transition temperatures in Table I show these to be close to those obtained by DSC. Transition temperatures obtained from the C-11 label are by contrast lower (see Table I), presumably because of the stronger partitioning of this label, causing larger perturbations in the gel phase. In spite of this latter disadvantage, the C-11 label has been used extensively to study the titration behavior, salt dependence, and hydration characteristics. This is simply because with this label it is possible to work with

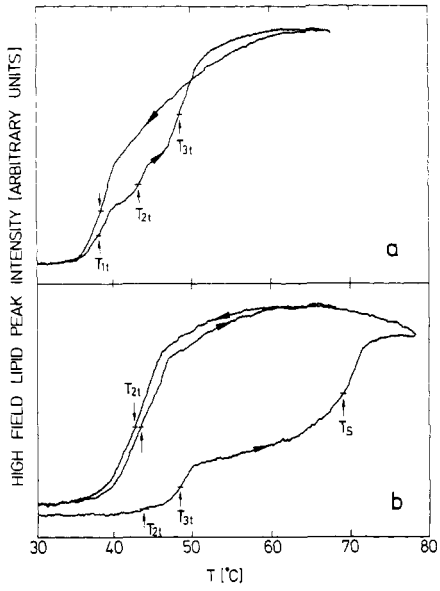

FIGURE 4: Composite phase transitions of partially hydrated DMPS in acidic buffers. (a) First heating scan and cooling scan of DMPS dispersed in buffer at pH ~2.4 and room temperature; (b) first heating and subsequent scans of DMPS mixed with buffer at pH 1.5 and room temperature. The dispersions contained 2.5 mM DMPS as the free acid, 75 μM C-11, and 10 μM EDTA, and the ionic strength was $J = 0.1$. Scanning rate, 2.5 °C min^{-1}.

much lower lipid concentrations, allowing much better definition of pH, salt concentration, etc. of the dispersions and giving less extensive lipid degradation at the extreme pH values. Although the label will be reliable in indicating systematic trends, it must be remembered that the absolute values of the transition temperature obtained with it must be corrected up to higher temperatures.

A typical temperature scan of the high-field lipid line of the C-11 label in DMPS bilayers at neutral pH is given in Figure 3b. A single transition is observed at 31 ± 1 °C with no hysteresis. Monitoring the high-field aqueous line in DMPS dispersions at high pH gave results as indicated in Figure 3c. On the upward scan a small pretransition at ~2 °C was observed before the main transition at 7 °C, and on the downward scan considerable hysteresis was seen, the main transition not occurring until around the (upward) pretransition temperature. Reversibility of the cycle was found on at least the first two complete scans, and TLC analysis indicated that the lipid remained >95% pure after the first cycle, provided the temperature did not exceed T_t by more than 5–10 °C.

The hydration behavior was complex for samples at low pH, and the results depended on sample preparation, as observed above for the DSC results. Samples made by hydrating the dry lipid in a small volume of water at 40 °C and then adding excess volume of the appropriate buffer $0.5 < \text{pH} < 3.2$ displayed a single transition at 39 °C. Samples prepared by dispersing dry lipid in low pH buffer and heating at $T > 85$ °C for 15 min also only gave a single transition at $T_t \simeq 39$ °C. If dry lipid was mixed with buffer $2.8 \leq \text{pH} \leq 3.8$ at room temperature, the transition was observed mainly at 43 °C on the first heating run and then at 39 °C for all subsequent scans (Figure 3d). Dispersing dry lipid in buffer pH ≲2.8 at room temperature gave rise to transitions in which most of the intensity was usually at $T_t \simeq 47$ °C on the first heating scan (Figure 3e,f). If the sample was heated to intermediate temperatures, the transition was observed at 43 °C on the downward scan in most cases (data not shown) or a coexistence of the 39 and 47 °C transitions (Figure 3e). On heating to

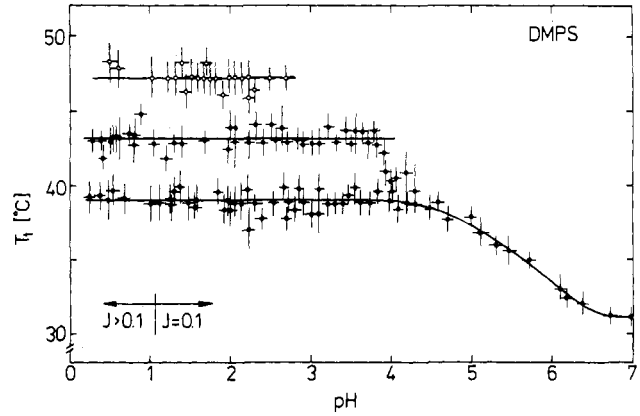

FIGURE 5: pH titration of the phase transition temperature of DMPS multibilayer dispersions in acidic buffers of constant ionic strength, $J = 0.1$. Transition temperatures are the mean of the heating and cooling data, obtained by monitoring the ESR line height of the C-11 spin-label in the lipid. (●) Transition temperatures of dispersions hydrated in small volumes of water and subsequently buffered or of dispersions made in the appropriate buffer and incubated at 90 °C for $t > 15$ min. (◑, The middle transition) Transition temperatures observed in the first heating (at low intensity) and in subsequent scans of dispersions which were not incubated at high temperature. (○) Transition temperatures seen solely in the first heating runs with samples in low-pH buffer.

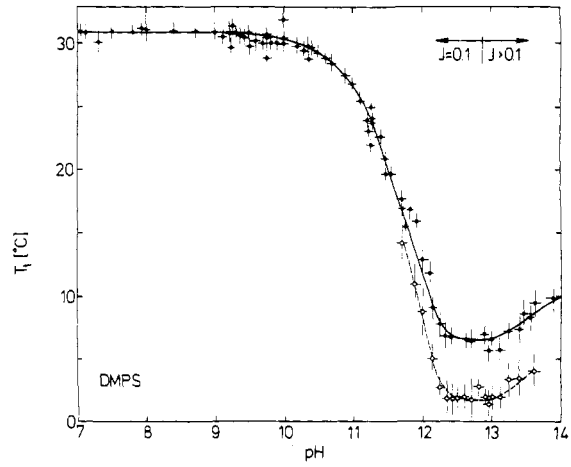

FIGURE 6: pH titration of the transition temperature of multibilayer dispersions in alkaline buffers of constant ionic strength, $J = 0.1$. The values at $7 \leq \text{pH} \leq 9.5$ are the means of determinations using the C-11 spin-label line height in the water and in the lipid, respectively. The values at $9.5 \leq \text{pH} \leq 14$ were determined only from the water line. Filled circles correspond to the main transition temperature, T_t, and open circles to the pretransition temperature, T_p. The buffers contained 10 μM EDTA, and the scanning rates were 5 °C min^{-1}.

higher temperatures, only the 39 °C transition was observed on the downward scan (Figures 3f and 4a).

In mixtures of dry PS with buffers of pH ≲2.8 (and often at $2.8 \leq \text{pH} \leq 4.0$), transitions were also observed at temperatures higher than $T_t \simeq 47$ °C (Figure 4b). These often appeared at 51–52, 55–56, and 60 °C, with most intensity in the highest one, which moved to higher temperatures on going to lower pH. Once the sample was heated through this high transition, it showed either only one transition, normally at $T_t \simeq 43$ °C (Figure 4b), or the 43 °C transition plus one lower transition at 39 °C (data not shown).

pH Titration of T_t. The pH dependence of the transition temperature recorded by the C-11 spin-label is given in Figures 5 and 6 for DMPS dispersions in buffers of constant ionic strength $J = 0.1$ over the range $1.1 < \text{pH} < 12.9$. Clear titrations are observed in the regions $pK_{app} \simeq 5.5$ and $pK_{app} \simeq 11.5$, corresponding to the disociation of the carboxyl and

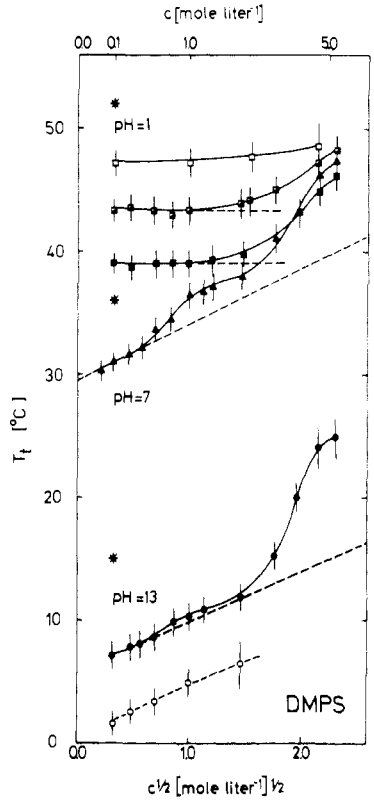

FIGURE 7: Effect of bulk monovalent ion concentration on the transition temperature of DMPS in different ionization states. (pH 1) Dispersion in 0.1 N HCl, 10 μM EDTA, and the appropriate amount of NaCl to yield the final monovalent ion concentration, c. (■) Dispersions hydrated in water or incubated at 90 °C for $t > 15$ min. (□) The first and (◪) subsequent scans with dispersions not incubated at high temperature. (pH 7) (▲) Dispersion in $(HOCH_2CH_2)_3N$·HCl/NaOH pH 7.0 buffer with appropriate amounts of NaCl. (pH 13) (●) Dispersions in buffers of pH 12.5 with appropriate amounts of NaCl (heating scans). The open circles correspond to the pretransition. All the determinations, except those denoted by (□) are the means of two temperature cycles. Asterisks represent the values measured by DSC with samples prepared in the same buffers. The dashed lines represent the T_t salt dependence as predicted by the Gouy–Chapman diffuse double layer theory.

amine groups, respectively. No shift in T_t which could be attributed to titration of the phosphate group was observed throughout the pH range studied. At low pH (Figure 5), three transition temperatures are indicated, corresponding to the different hydration states discussed in the previous section. For fully hydrated bilayers the transition temperature measured by the C-11 label increases from 31 to 39 °C on protonating the head-group carboxyl. At high pH the transition temperature decreases to 7 °C, with a pretransition at 2 °C, on deprotonating the amine group. The increase in transition temperature of charged PS bilayers at pH >13 is caused by the screening of the surface charge due to the higher ionic strength of the buffers used in this pH range.

Salt Dependence of T_t. For determination of the electrostatic contribution to the transition temperature titration, T_t was measured as a function of ionic strength [cf. Cevc et al. (1980)]. The dependence of T_t (as measured by the C-11 label) on salt concentration is given in Figure 7, for DMPS in the three different charge states of its titration. At pH 7, where the PS is in the singly negatively charged state, T_t increased with increasing salt concentration, at first approximately linearly with $c^{1/2}$, then less rapidly, flattening off apparently to a first saturation value at a salt concentration $c \simeq 2$ M, and then rapidly again at higher salt concentrations. The highest concentration points on Figure 7 correspond to

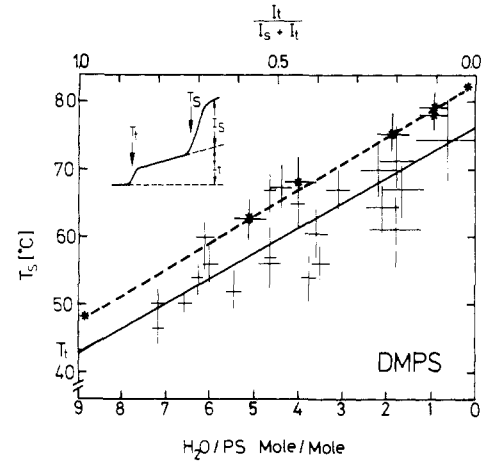

FIGURE 8: Hydration dependence of the DMPS bilayer phase transition. The asterisks and dashed line represent DSC results on DMPS/water mixtures of varying molar ratios, which were determined gravimetrically. The crosses (error bars) and full line represent spin-label measurements on partially hydrated samples in buffers (J = 0.1) with 1.0 ≤ pH ≤ 3.8; the relative hydration $I_t/(I_t + I_s)$ and the transition temperature, T_s, are defined in the insert. The lines represent linear regression fits to the data points.

a saturated solution of NaCl (at 20 °C), ~6 M.

At pH 12.5–13, PS is in the doubly negatively charged state, and T_t again increased with increasing ionic strength. The transition temperature had not completely plateaued at c = 2 M, at which point it increased rapidly again, as observed at pH 7. The pretransition also increased with increasing salt concentration and finally disappeared at $c \simeq 2$ M.

At pH ≤2.8, PS is in its zwitterionic state, and T_t showed no marked dependence on salt concentration for all three different hydration states, up to $c \simeq 2$ M. Above c = 2 M, T_t began to increase with increasing salt concentration, and all three transitions appeared to approach a similar value in saturated salt solution.

Hydration Dependence of T_t. The transition temperature of DMPS as a function of water content, measured by DSC, is given in Figure 8. An approximately linear dependence is observed which reaches the value of fully hydrated bilayers at pH 1.0, $T_{2t} \simeq 48$ °C, at an estimated hydration of ~9 water molecules/PS molecule. This hydration dependence is mirrored by the transition behavior of DMPS in the low-pH buffers, measured by the C-11 label, as discussed earlier (Figure 4b). Plotting the high-temperature transition (cf. Figure 4b, $T_s \simeq 70$ °C) against the relative intensity of the low-temperature transition $I_t/(I_t + I_s)$ as indicated in the inset to Figure 8, yields a nearly parallel dependence to the hydration dependence. This linear dependence extrapolates to $T_{2t} \simeq 43$ °C in agreement with the value obtained for the hydrated sample on the downward temperature scan (Figure 4b). The correlation between the two curves in Figure 8 supports the previous conclusion that the various different transition effects observed in low-pH buffers are due to incomplete hydration.

Discussion

The results given in the previous section represent a rather complete study of the titration of the phase transition of phosphatidylserine bilayers. Previous studies (MacDonald et al., 1976; van Dijck et al., 1978) have concentrated solely on the carboxyl group titration and thus have not observed the large decrease in transition temperature at the amino group titration, or the occurrence of the pretransition at high pH. In addition, the problems with hydration at low pH were not

fully realized. Thus, the T_t (pH 1) = 54.8 °C obtained by van Dijck et al. (1978) for DMPS and T_t (pH ~2.5) ≃ 72 °C obtained by MacDonald et al. (1976) for DPPS are even greater than the highest values reported here by DSC of T_{3t} = 52 and 68.5 °C for DMPS and DPPS, respectively. This strongly suggests that the former measurements refer to samples with less than maximum hydration.

It should be noted that the absolute values of T_t obtained with the C-11 label are systematically ~5–7 °C lower than those found by DSC. Whereas it was impracticable (for reasons given under Results) to perform such exhaustive studies with DSC as with spin-labels, all qualitative features of the PS phase behavior discovered by spin-label measurements were confirmed by DSC.

Electrostatic Contributions to T_t: Salt Dependence. The screening of the surface potential by salt has previously been used to isolate the electrostatic contribution to the phase transition temperature of phosphatidylglycerol bilayers (Cevc et al., 1980). From Figure 7 it can be seen that in the low-pH region T_{1t}, T_{2t}, and T_{3t} are independent of electrolyte ionic strength in the range 0.1–1.5. In the neutral pH range, such an increase in ionic strength effectively eliminates the surface potential of PS bilayers (Eisenberg et al., 1979; Nir & Benz, 1978). Thus it appears, as expected, that there is no contribution to T_t from an electrostatic surface potential in the zwitterionic state at low pH, and it can be automatically excluded that the existence of the three T_t's (T_{1t}, T_{2t}, and T_{3t}) arises from different ionization states.

A salt dependence of T_t first appears at $3.0 \leq$ pH ≤ 6.5, i.e., in the titration region of the carboxyl group. In contrast to the findings of MacDonald et al. (1976), we observe a well-defined ionic dependence of the transition temperature of singly negatively charged PS [Figure 7 (▲)]. At pH 7, well above the titration region, the transition temperature increases from T_t^- (J = 0.1) = 36 °C to T_t^- (J = 1.5) = 43.5 °C as observed by DSC (from 31 to 39 °C by C-11 ESR). Such a salt-induced increase in T_t is consistent with a lowering of the transition temperature by the electrostatic surface charge (Träuble & Eibl, 1974). The maximum electrostatic contribution to the transition temperature shift is given by Gouy–Chapman diffuse double-layer theory to be (Träuble et al., 1976)

$$\Delta T_{tm}^{el} = -(2kTN_A/\Delta S_t^*)\Delta f_c/f_c \qquad (1)$$

where the high-potential approximation, $|e\psi_0| \gg kT$, is assumed, k, T, N_A, and e have their usual meanings, ΔS_t^* is the transition entropy of the *un*charged bilayer, and $\Delta f_c/f_c$ is the relative increase in the area *per charge*, f_c, at the transition. The salt-induced screening of the double-layer potential decreases ΔT_{tm}^{el} to ΔT_t^{el} by an amount given by (Träuble et al., 1976):

$$\Delta T_{tm}^{el} - \Delta T_t^{el} = [4\epsilon\epsilon_0 N_A k^2 T^2/(e^2\Delta S_t^*)]\Delta f_c \kappa \qquad (2)$$

where ϵ and ϵ_0 denote the relative permittivities of the interfacial region and of free space, respectively, and κ is the reciprocal Debye screening length, $\kappa = (2000N_A e^2 c/\epsilon\epsilon_0 kT)^{1/2}$, which is proportional to the square root of the bulk ion concentration, c. The data of Figure 7 show an initial linear dependence on $c^{1/2}$ at pH 7, with slope $dT_t/dc^{1/2} \simeq 4.4$ °C $L^{1/2}$ $mol^{-1/2}$. At higher salt concentrations ($c > 0.5$) the screening is stronger than predicted by Gouy–Chapman theory with indications of leveling off at c = 1–2 M. In comparison with similar results on phosphatidylglycerol (Cevc et al., 1980) and electrophoretic measurements on PS (Eisenberg et al., 1979), it is suggested that this leveling off corresponds to the complete screening of the surface potential, and thus ΔT_{tm}^{el} ≃ −7.5 °C. Additional evidence for this assumption comes from the fact that the plateau values of T_t at pH 7 lie close to the T_t of the fully hydrated zwitterionic state at pH 1, suggesting that the whole of the transition temperature shift at the carboxyl group titration $\Delta T_t \simeq -8$ °C, arises from electrostatic effects. At higher concentrations ($c > 2$ M) the transition temperature increases rapidly with increasing salt, irrespective of the charge state of the lipid. This sharp change is attributed to specific ion binding, the increase in T_t most probably being due to displacement of water of hydration, as discussed later.

If $\epsilon \simeq 50$ in the electrostatic double layer (Grahame, 1950) is assumed, the experimental value of $dT_t/dc^{1/2}$ at pH 7.0 is consistent with eq 2 if a value of $\Delta f_c = 0.13$ nm^2 is taken for the expansion in area per charge at the phase transition. Using this value in eq 1 it is found that the pH 7 value of ΔT_{tm}^{el} would require a value $f_c = 0.98$ nm^2 for the mean area per charge. This latter value is almost certainly too large, a value of $f_c \simeq 0.45$–0.55 nm^2 would be more appropriate on the basis of X-ray results (Janiak et al., 1976; Harlos, 1978). Thus the simple Gouy–Chapman diffuse double-layer theory both fails to account for the electrostatic screening at moderate salt concentrations and to give a consistent interpretation of the magnitudes of the maximal transition temperature shift and the rate of screening at low salt concentration.

The results in the doubly charged state at pH 13 [Figure 7 (●)] are qualitatively similar to those at pH 7, although the deviations from a linear dependence on $c^{1/2}$ at moderate salt concentrations are less. The initial salt dependence gives $dT_t/dc^{1/2} = 3.4$ °C $L^{1/2}$ $mol^{-1/2}$, and at $c \simeq 2$ M, $\Delta T_{tm}^{el} \simeq -6$ °C. This would require values of $\Delta f_c = 0.11$ nm^2 and $f_c = 1.02$ nm^2 for agreement with double-layer theory. Again simple Gouy–Chapman theory does not account for the observed electrostatic shifts (nor does the electrostatic shift account for the whole of the shift, $\Delta T_t \simeq -21$ °C (DSC), between pH 7 and pH 13). A better description of the electrostatic and ionic effects would require taking into account the discreteness of charge (Grahame, 1958), ion binding (McLaughlin, 1977), the effect of vicinal water (Radič & Marčelja, 1978), and the changes in transverse mobility of the head groups (Cevc et al., 1981).

In summary, the salt dependence in the different charge states indicates that there is no electrostatic surface charge contribution to T_t in the zwitterionic state at pH 1. The measured shift, $\Delta T_t = -8$ °C titration from pH 1 to the singly charged state at pH 7 can be accounted for solely in terms of electrostatics. However, the very large shift, $\Delta T_t = -21$ °C, on titration from pH 7 to the doubly charged state at pH 13 cannot be accounted for solely by surface electrostatics. The electrostatic contribution to this shift is estimated to be approximately $\Delta T_{tm}^{el} \simeq -6$ °C.

Dissociation Properties of PS Bilayers. The apparent dissociation constants of the DMPS bilayers, as deduced from the midpoints of the transition temperature titrations in Figures 5 and 6, are given in Table II. As seen from Figure 5, no titration is observed for the phosphate group in fully hydrated bilayers at pH >0.5. This is in agreement with the results at low pH of other workers (cf. Table II). The apparent step which occurs between T_{2t} and T_{3t} at pH ~2.6 in Figure 5 may possibly be associated with some change in the phosphate moiety, since it occurs well below the titration range of the carboxyl group. However, the T_{3t} transition occurs only in samples with less than maximum hydration, and, as shown in the next section, it is most probable that the difference between T_{3t} and T_{2t} corresponds to a change in hydration. For this

Table II: Apparent Dissociation Constants of Phosphatidylserine Bilayers

pK_1^i	pK_2^i	pK_3^i	lipid characteristics	remarks; method[b]	ref
<0.5	5.5	11.55	DMPS, multibilayers	$J = 0.1$, 10 μM EDTA; T_t(pH)	this work
(2.60)[c]			DMPS, precipitate	not fully hydrated; T_t(pH)	
	4.4		DMPS, centrifuged wet pellet	0.1 M NaCl, 25 mM Pipes; T_t(pH)	*d*
	4.6		DPPS, injection vesicles, $T < T_t$	0.1 M NaCl; T_t(pH)	*e*
	3.5		DPPS, injection vesicles, $T > T_t$	0.1 M NaCl; acid–base titration	
	4.24		BBPS, multilayers	0.1 M KCl, 0.1 mM EDTA; phase separation	
<3.6			BBPS, sonicated vesicles	0.1 M KCl, 0.1 mM EDTA; ^{31}P NMR	*f*
	4.3	10.0	spinal cord PS, sonicated vesicles	0.13 M KCl; electrophoretic mobility	*g*
	4.42	9.93	BBPS, sonicated vesicles	0.1 M $(C_3H_7)_4NI$; acid–base titration	*h*
	3.20	9.70	BBPS, sonicated vesicles	0.5 M NaCl; acid–base titration	*i*
	4.6	10.3	BBPS, mixed solvent	2-ethoxyethanol–1% H_2O, 10^{-3} M KCl; acid–base titration	*j*
(<1)[a]	(2.65)[a]	(9.99)[a]	phosphoserine, in H_2O	acid–base titration	*k*

[a] Intrinsic pK_i^w of phosphoserine in bulk aqueous solution. The additional phosphate pK ($RHPO_4^-$) is 5.91 (Neuhaus & Korkes, 1958). [b] T_t(pH) refers to titration of the bilayer phase transition temperature. [c] Corresponds to the appearance of T_{3t}, but does not resemble a true titration curve. [d] van Dijck et al. (1978). [e] MacDonald et al. (1976). [f] Tokutomi et al. (1980). [g] Hauser et al. (1975). [h] Hendrickson & Fullington (1965). [i] Abramson et al. (1964). [j] Garvin & Karnovsky (1956). [k] Neuhaus & Korkes (1958).

reason the value of $pK_1^i \simeq 2.6$, is given in parentheses in Table II.

The apparent pK of the carboxyl group, $pK_2^i = 5.5$, is significantly higher than those values obtained for PS bilayers by other workers: $pK_2^i \simeq 4.5$ (Table II). Part of the reason for this discrepancy is almost certainly the difficulty in hydration at low pH. If T_{2t} or T_{3t}, rather than T_{1t}, is taken as the end point of the titration, then the pK_2^i will appear to be biased to lower pHs. Thus the higher value is the more appropriate for the fully hydrated bilayers.

The apparent pK of the amino group, $pK_3^i = 11.55$, is also significantly larger than those reported previously (see Table II). Again electrostatic (upward) shifts are expected to be greater for DMPS than for BBPS and spinal cord PS, although polarity-induced shifts are in the opposite directions (see below). Confirmation of our pK_a value comes from a similar titration of DMPE which gave a pK_2^i(PE) = 11.25, 0.3 pH unit lower than that for PS as might be expected from the reduced electrostatic surface charge [cf. also Stümpel et al. (1980)].

The apparent pK_i^i of a group at the bilayer interface differs from the intrinsic pK_i^w of the group in bulk water, due to the electrostatic enhancement of the hydrogen ion concentration (activity) at the interface, induced by the surface charge, and also due to the shift in the acid–base equilibrium arising from the different local polarity at the interface (Fernández & Fromherz, 1977)

$$pK_i^i = pK_i^w + \Delta pK_i^{el} \pm |\Delta pK_i^p| \quad (3)$$

where ΔpK_i^{el} is the electrostatic-induced shift and ΔpK_i^p is the polarity-induced shift. The sign of the polarity-induced shift depends on the change in total number of charges on protonation. For the dissociation of a molecular acid, the pK is increased as a result of the lower dielectric permittivity at the interface than in bulk solution, whereas for the dissociation of a cationic acid the reverse is true.

The electrostatic shift in pK is

$$\Delta pK_i^{el} = -e\psi_0/(2.3kT) \quad (4)$$

If the surface potential, ψ_0, is calculated from the high-potential approximation of diffuse double-layer theory

$$\Delta pK_i^{el} = \log [e^2/(8000 N_A kT\epsilon\epsilon_0 f_c^2 c_0)] - \log (c/c_0) \quad (5)$$

where $c_0 = 1$ M and c is the molar concentration of electrolyte, all the other quantities being in SI units.

Because PS forms bilayers spontaneously in water, it is not possible to measure the intrinsic monomer pKs directly. If we assume that the pK_i^ws can be identified with those for phosphoserine, then we obtain ΔpK_2^i ($=pK_2^i - pK_2^w$) = 2.85 and $\Delta pK_3^i = 1.56$ from Table II, for the total pK shifts in DMPS bilayers. The fact that $\Delta pK_2^i > \Delta pK_3^i$ immediately indicates that there must be polarity-induced pK shifts at the DMPS bilayer interface, since the electrostatic shifts will be greater for pK_3, because of the greater surface charge (cf. eq 3–5). The change in charge state at pK_2 can be designated $(-+) \rightarrow (--+)$, corresponding to an increase in the number of charges, whereas that at pK_3 is $(--+) \rightarrow (--)$, corresponding to a decrease in the total number of charges. Hence a decreased dielectric permittivity at the interface will contribute a positive polarity-induced shift to pK_2 and a negative one to pK_3, which is totally consistent with the inequality observed above. If it is assumed, following Fernandez & Fromherz (1977), that $\epsilon \simeq 30$ at the interface, then $\Delta pK_2^p \simeq +1.1$ and $\Delta pK_3^p \simeq -1.1$. Hence the electrostatic shifts for DMPS, calculated from eq 3 would be $\Delta pK_2^{el} = 1.75$ and $\Delta pK_3^{el} = 2.66$, corresponding to surface potentials of $\psi_0(pK_2) \simeq -109$ mV and $\psi_0(pK_3) \simeq -158$ mV, respectively. The value of ψ_0 at pK_2 is smaller than that at pK_3 because of the lower net surface charge density. Calculations from Gouy–Chapman theory, using eq 5 and assuming $\epsilon \simeq 30$, show that these surface potentials can be accounted for with areas *per molecule* of $f_{mol}(pK_2) \simeq 0.46$ nm^2 and $f_{mol}(pK_3) \simeq 0.48$ nm^2. The agreement between these two values, and with those expected on the basis of X-ray results (see above), is satisfying (although one might possibly expect the bilayers at pK_3 to be more expanded than those at pK_2, as a result of the larger surface charge).

In summary, the dissociation data indicate that the DMPS bilayer–aqueous interface has a lower polarity than in bulk solution, corresponding to $\epsilon \simeq 30$, and the electrostatic-induced pK shifts indicate that the bilayer surface potential is approximately −100 mV at T_t at pK_2, and approximately −150 mV at T_t at pK_3.

PS Bilayer Hydration. The complicated dependence of the transition temperature on sample prehistory at low pH has already been discussed under Results. This, together with the water dependence of T_t in Figure 8, gives valuable information

Table III: Type and Number of Water Molecules Associated with Phosphatidylserine Bilayers

bound water			trapped water	lipid	remarks	ref
PO_4^-	NH_3^+	COO^-				
9-8	0-1	1		DMPS	$J = 0.1$, $T \leq T_t$	this work
8-7	0-1	0		DMPS	saturated NaCl, $T < T_t$	
——— 12 ———			120	NaBBPS	D_2O NMR, $T > T_t$	Finer & Darke (1974)
——— ≤8 ———			140	NaBBPS	X-ray diffraction	Hauser et al. (1977)

on the hydration of the PS head group. The DSC results on water dependence in Figure 8 indicate that the PS bilayers at low pH reach a limiting hydration of 9 H_2O molecules/PS molecule, above which the transition temperature is independent of water content. Up to this value the transition temperature decreases by ~4 °C/H_2O molecule added to the lipid–water mixture. The correlation with the behavior in the first upward temperature scan of DMPS dispersed in excess buffer of low pH, shown in Figure 8, strongly indicates that the coexistence of different transitions arises from the difficulty of hydration at low pH. Although the spread of the data is quite large, the temperature of the higher (less hydrated) transition, T_s, correlates rather well with the fraction of the lipid in the fully hydrated state as measured by the ratio of intensity of the first transition, T_{2t}, to that of all transitions, T_{2t} and T_s. The validity of this comparison is also strongly supported by the fact that the extrapolated value of T_s for zero hydration, corrected for the spin-label perturbation effect, yields approximately the same value for the anhydrous transition temperature as is measured by DSC.

From these results it can be inferred that the three different transition temperatures, T_{1t}, T_{2t}, and T_{3t}, and transition enthalpies observed for samples at low pH (see Figure 5 and Table I) most probably correspond to different states of head-group hydration. The lack of any salt dependence between $J = 0.1$ and $J = 2.0$ rules out the possibility of an electrostatic origin for these differences, as already noted. The magnitudes of the differences in transition temperatures, $T_{1t} - T_{2t} \simeq T_{2t} - T_{3t} \simeq -4$ °C, suggests that these correspond to hydration states differing by one water molecule (cf. Figure 8). Supporting evidence for the idea that T_{1t}, T_{2t}, and T_{3t} correspond to different states of hydration comes from the behavior at high ionic strength. As the bulk monovalent ion concentration is increased above 2.5 M, the difference between the three transition temperatures decreases, as does the difference between these and T_t^- (see Figure 7). Both NMR experiments (Hauser et al., 1975) and theoretical calculations (Gresh, 1980) suggest that water molecules and ions have a preference for the same sites on the PS polar head groups. Indeed, Ca^{2+} is able to form anhydrous complexes with PS (Hauser et al., 1977; Newton et al., 1978). Thus it seems likely that at high salt concentrations the ions compete with water molecules for certain binding sites on the polar head group and screen the differences between the different states of hydration. The steep increases in transition temperature at high ionic strength would then be due to partial displacement of water molecules by ion binding.

The difficulty in hydration of PS first arises during the protonation of the carboxyl group, and indeed the state associated with T_{1t} corresponding to complete hydration of the protonated carboxyl group is only achieved with considerable difficulty. Thus, the change from the state with transition temperature T_{1t} to that with transition temperature T_{2t} most probably corresponds to the loss of a water molecule associated with the carboxyl group, on protonation of the latter. In this connection it is interesting to note that T_{2t} corresponds closely to the T_t of phosphatidylethanolamine which differs from PS only by the lack of the carboxyl group. Moreover, the transition enthalpies of the two lipids are similar.

The degree of hydrophobicity of the PS polar head group increases on going to even lower pHs, and the state of lower hydration corresponding to T_{3t} does not appear until pH ≤2.8 which is well below the pK of the carboxyl group. Thus it appears that most of the water molecules of hydration are associated with the phosphate group. This is consistent with current views on the hydration properties of phospholipids (Hauser & Phillips, 1979) and also with the data of Schumacher & Sandermann (1976), who found a much greater hydration of the sodium salt of DL-phosphoserine than of the free acid. Evidence for strong association of water with the phosphate group and relatively little association with the amino group comes from theoretical studies on the hydration of model compounds for polar head-group segments (Port & Pullman, 1973; Frischleder et al., 1977). It was found in these latter two studies that the binding energy for water molecules to dimethyl phosphate is 108.8 (25.9) kJ (kcal)/mol for the first water molecule, decreasing to 43.3 (10.3) kJ (kcal)/mol for the seventh water molecule, whereas the binding energy to tetramethylammonium is only 43.3 (10.3) kJ (kcal)/mol for the first water molecule.

Our conclusions regarding the hydration of DMPS are summarized in Table III, which also gives a comparison of the present results with those of previous studies. It is concluded that hydration plays an important role at the carboxyl titration but not at that of the amino group.

Hydrogen Bonding of PS Head Groups. It has previously been suggested that the breaking or weakening of *inter*molecular hydrogen bonds could contribute to the titration-induced shift of the bilayer phase transition (Nagle, 1976; Eibl & Woolley, 1979). Since the transition temperature shift at the carboxyl titration is fully accounted for by the electrostatic and hydration effects, it seems that the hydrogen-bonding capacity of this group must be satisfied either by *intra*molecular hydrogen bonds or by hydrogen bonds with water. MacDonald et al. (1976) had previously proposed a hydrogen-bond contribution to the carboxyl titration, based on a lack of salt dependence of T_t at neutral pH. However, our more detailed experimental results on the salt dependence given in Figure 7 show this not to be the case.

As seen from Figure 7, however, the major part of the transition temperature shift induced by titration of the amino group cannot be accounted for by either electrostatic or hydration effects. Comparison with DMPE which also has similar shifts (data not shown) eliminates the possibility of sizable dipolar contributions. This points to the existence of a strong, specific *inter*molecular force involving the amino group, most probably hydrogen bonding. The NH_3^+ group is an extremely good proton donor, whereas the neutral amino group can be a hydrogen-bond acceptor (e.g., in arginine or purine and pyrimidine bases). The deprotonation of the NH_3^+ group thus necessarily causes a weakening (if not breaking) of any direct bonds which involve this group as proton donor.

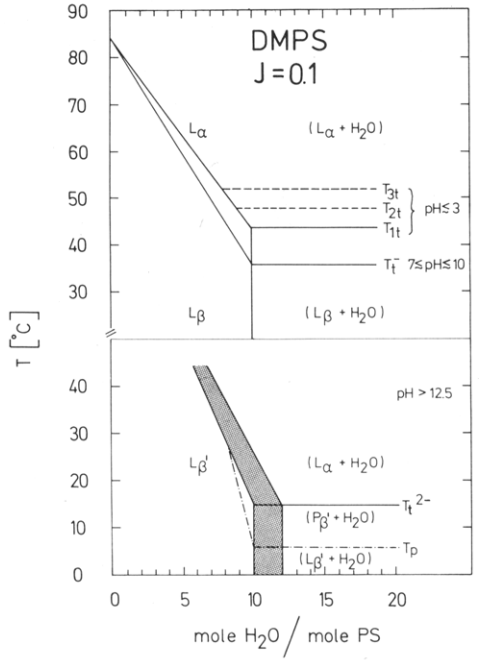

FIGURE 9: Proposed phase diagrams of DMPS bilayers in the various states of hydration, based on transition temperature measurements as a function of hydration and pH. The abscissa indicates the molar ratio of H_2O/PS in the mixture. The assignment of the different phases is made by comparison with the phase behavior of other phospholipids for which the structure has been determined. (Upper) Composite phase diagram for pH $\lesssim$3 and 7 $\lesssim$ pH $\lesssim$ 10. The phase boundaries for the two different protonation states are projected onto a single diagram. The dashed lines at pH $\lesssim$3 indicate the phase boundary at the two states (T_{2t}, T_{3t}) of lower hydration. Above each line the bilayer is in the L_α phase, and below is in the L_β or $L_{\beta'}$ phase. (Lower) Phase diagram for pH >12.5; the broad lines indicate the uncertainty in the exact water dependence at high pH.

If it is assumed that the electrostatic contribution to the amino group titration T_t shift is screened out in saturated salt solution, the maximum hydrogen bonding contribution to the shift is $\Delta T_t^{HB}(NH_3^+) = -22$ °C (see Figure 7). It is difficult to say whether this shift is due entirely to the weakening or breaking of hydrogen bonds or due partly to some secondary effect of the hydrogen-bond disruption. In energetic terms a shift of this magnitude could easily be accounted for directly by hydrogen bonding (Nagle, 1976; Eibl & Woolley, 1979) but not, for instance, by double-layer electrostatics. It has previously been suggested that a change in the angle of tilt of the lipid chains in the ordered phase could contribute to the transition temperature shift (Jähnig et al., 1979). It seems quite likely that the PS chains are tilted in the ordered phase at pH 13 since PS shows a pretransition at high pH. However, the tilt contribution presumably arises from changes in head-group interactions including hydrogen bonding, rather than solely from surface charge effects as originally suggested for phosphatidic acid (Jähnig et al., 1979), since neither a tilt contribution to the transition temperature shift nor a pretransition is observed in the singly charged state at pH 7. Thus part, but almost certainly not all, of the titration shift at high pH may be due to chain tilt as an indirect effect of hydrogen bond disruption.

Phase Behavior of PS. Most of the results of this study can be summarized in the generalized phase diagram for DMPS presented in Figure 9. The phase boundaries in this diagram are constructed from the water dependence of the phase transition temperatures in the various ionization states of PS. The identification of the various phases is made by comparison with the phase behavior of other lipids for which the phases have been previously defined [see, e.g., Janiak et al. (1976, 1979)].

The transition of the anhydrous lipid occurs at 84 ± 2.5 °C (89 ± 2.5 °C for DPPS). By comparison with the results for other anhydrous lipids (Finean, 1956; Ladbrooke & Chapman, 1969; Harlos & Eibl, 1980), it can be concluded that the lipid chains melt at this temperature, rather than the lipid as a whole as was previously assumed (MacDonald et al., 1976). The capillary melting point of our DMPS preparations was 163–165 °C (159–161 °C for DPPS), in agreement with the original result of Baer & Maurukas (1955). The high-temperature phase can thus be identified as L_α and, by analogy with other lipids, the low-temperature phase is identified as being one of the L_β types (Tardieu et al., 1973; Janiak et al., 1976). As the water content is increased, the transition temperature decreases, reaching a limiting value at 9–10 water molecules/PS molecule, as was indicated in Figure 8. Beyond this value the excess water will be present essentially as a free phase. The limiting value of the transition temperature at maximum hydration is ~8 °C lower at neutral pH than at low pH, and at low pH there are at least two states, each ~4 °C higher in transition temperature, corresponding to bilayers with progressively 1 water molecule of hydration less/PS molecule.

At high pH, not only is a main transition observed but also there is a pretransition lying at ~9–10 °C (6–7 °C by ESR) below the main transition. Both the absolute and the relative magnitudes of the enthalpies of the main transition and the pretransition are similar to those obtained previously for phosphatidylcholines (Ladbrooke & Chapman, 1969; Hinz & Sturtevant, 1972). Thus, it seems likely that the phase behavior may be similar to that of phosphatidylcholines, namely, a tilted $L_{\beta'}$ phase existing below the pretransition and a rippled $P_{\beta'}$ phase in the intermediate region between the pre- and main transitions [cf. Janiak et al. (1976, 1979)]. The enthalpies of the main transition in the two other pH regions are also similar to those for phosphatidylcholines, again suggesting that these correspond to normal lamellar bilayer phases.

Acknowledgments

We thank B. Hirche for her expert assistance in preparation of the phosphatidylserine and Dr. K. Harlos for his advice with the differential scanning calorimetry.

References

Abramson, M. B., Katzman, R., & Gregor, H. P. (1964) *J. Biol. Chem. 239*, 70–76.

Baer, E., & Maurukas, J. (1955) *J. Biol. Chem. 212*, 25–48.

Browning, J. L., & Seelig, J. (1979) *Chem. Phys. Lipids 24*, 103–118.

Cevc, G., Watts, A., & Marsh, D. (1980) *FEBS Lett. 120*, 267–270.

Cevc, G., Svetina, S., & Žekš, B. (1981) *J. Phys. Chem. 85*, 1762–1767.

Comfurius, P., & Zwaal, R. F. A. (1977) *Biochim. Biophys. Acta 488*, 36–42.

Eibl, H., & Woolley, P. (1979) *Biophys. Chem. 10*, 261–271.

Eisenberg, M., Gresalfi, T., Riccio, T., & McLaughlin, S. (1979) *Biochemistry 18*, 5213–5223.

Ferñandez, M. S., & Fromherz, P. (1977) *J. Phys. Chem. 81*, 1755–1761.

Finean, J. B. (1953) *Biochim. Biophys. Acta 10*, 371–384.

Finer, E. G., & Darke, A. (1974) *Chem. Phys. Lipids 12*, 1–16.

Frischleder, H., Gleichmann, S., & Krahl, R. (1977) *Chem. Phys. Lipids 19*, 144–149.

Garvin, J. E., & Karnovsky, M. L. (1956) *J. Biol. Chem. 221*, 211–222.
Grahame, D. C. (1950) *J. Chem. Phys. 18*, 903–909.
Grahame, D. C. (1958) *Z. Elektrochem. 62*, 264–274.
Gresh, N. (1980) *Biochim. Biophys. Acta 597*, 345–357.
Harlos, K. (1978) *Biochim. Biophys. Acta 511*, 348–355.
Harlos, K., & Eibl, H. (1980) *Biochemistry 19*, 895–899.
Hauser, H., & Phillips, M. C. (1979) *Prog. Surf. Membr. Sci. 13*, 297–413.
Hauser, H., Phillips, M. C., & Barratt, M. D. (1975) *Biochim. Biophys. Acta 413*, 341–353.
Hauser, H., Finer, E. G., & Darke, A. (1977) *Biochem. Biophys. Res. Commun. 76*, 267–274.
Hendrickson, H. S., & Fullington, J. G. (1965) *Biochemistry 4*, 1599–1605.
Hinz, H.-J., & Sturtevant, J. M. (1972) *J. Biol. Chem. 247*, 6071–6075.
Jacobson, K., & Papahadjopoulos, D. (1975) *Biochemistry 14*, 152–161.
Jähnig, F., Harlos, K., Vogel, H., & Eibl, H. (1979) *Biochemistry 18*, 1459–1468.
Janiak, M. J., Small, D. M., & Shipley, G. G. (1976) *Biochemistry 15*, 4575–4580.
Janiak, M. J., Small, D. M., & Shipley, G. G. (1979) *J. Biol. Chem. 254*, 6068–6078.
Ladbrooke, B. D., & Chapman, D. (1969) *Chem. Phys. Lipids 3*, 304–356.
MacDonald, R. C., Simon, S. A., & Baer, E. (1976) *Biochemistry 15*, 885–891.
Marsh, D., & Watts, A. (1981) in *Liposomes from Physical Structure to Therapeutic Applications* (Knight, C. G., Ed.) Chapter 5, Elsevier/North-Holland, Amsterdam.
McLaughlin, S. (1977) *Curr. Top. Membr. Transp. 9*, 71–144.
Melchior, D. L., & Steim, J. M. (1976) *Annu. Rev. Biophys. Bioeng. 5*, 205–238.
Nagle, J. F. (1976) *J. Membr. Biol. 27*, 233–250.
Neuhaus, F. C., & Korkes, S. (1958) *Biochem. Prep. 6*, 75–79.
Newton, C., Pangborn, W., Nir, S., & Papahadjopoulos, D. (1978) *Biochim. Biophys. Acta 506*, 281–287.
Nir, S., & Bentz, J. (1978) *J. Colloid Intface Sci. 65*, 399–414.
Papahadjopoulos, D. (1978) *Cell Surf. Rev. 5*, 765–790.
Port, G. N. J., & Pullman, A. (1973) *Theor. Chim. Acta 31*, 231–237.
Radič, N., & Marčelja, S. (1978) *Chem. Phys. Lett. 55*, 377–379.
Rozantzev, E. G., & Neiman, M. B. (1964) *Tetrahedron 20*, 131–137.
Schumacher, G., & Sandermann, H., Jr. (1976) *Biochim. Biophys. Acta 448*, 642–644.
Stümpel, J., Harlos, K., & Eibl, H. (1980) *Biochim. Biophys. Acta 599*, 464–472.
Tardieu, A., Luzzati, V., & Reman, F. C. (1973) *J. Mol. Biol. 75*, 711–733.
Tokutomi, S., Ohki, K., & Ohnishi, S. (1980) *Biochim. Biophys. Acta 596*, 192–200.
Träuble, H. (1971) *Biomembranes 3*, 197–227.
Träuble, H. (1976) *Nobel Symp. No. 34*, 509–550.
Träuble, H., & Eibl, H. (1974) *Proc. Natl. Acad. Sci. U.S.A. 71*, 214–219.
Träuble, H., Teubner, M., Woolley, P., & Eibl, H. (1976) *Biophys. Chem. 4*, 319–342.
van Dijck, P. W. M., de Druijff, B., Verkleij, A. J., van Deenen, L. L. M., & de Gier, J. (1978) *Biochim. Biophys. Acta 512*, 84–96.
Verkleij, A. J., de Kruijff, B., Ververgaert, P. H. J. Th., Tocanne, J. F., and van Deenen, L. L. M. (1974) *Biochim. Biophys. Acta 339*, 432–437.
Watts, A., Harlos, K., Maschke, W., & Marsh, D. (1978) *Biochim. Biophys. Acta 510*, 63–74.
White, D. A. (1973) *BBA Libr. 3 (2nd Ed.)*, 441–482.

Stabilization of the Red Semiquinone Form of Pig Kidney General Acyl-CoA Dehydrogenase by Acyl Coenzyme A Derivatives†

John P. Mizzer and Colin Thorpe*

ABSTRACT: Pig kidney general acyl-CoA dehydrogenase forms the blue neutral radical on dithionite or photochemical reduction [Thorpe, C., Matthews, R. G., & Williams, C. H. (1979) *Biochemistry 18*, 331–337] in accord with its classification as a flavoprotein dehydrogenase. However, dithionite reduction of the enzyme in the presence of crotonyl coenzyme A (crotonyl-CoA) or octenoyl-CoA generates the red radical anion as the predominant species at pH 7.6. Crotonyl-CoA binds preferentially to the red radical form, depressing the apparent p*K* by at least 2.5 pH units to a value of 7.3. Butyryl-, octanoyl-, and palmitoyl-CoA induce very similar spectral changes to those induced by enoyl-CoA derivatives when added anaerobically to the blue semiquinone enzyme. In contrast, the competitive inhibitors acetoacetyl-CoA and heptadecyl-SCoA do not markedly perturb the spectrum of the neutral flavosemiquinone species. The stability of the enzyme radical complexes with either crotonyl- or octanoyl-CoA suggests that there is not effective intraflavin transfer of reducing equivalents between subunits. Perturbation of the spectrum of the one-electron-reduced enzyme by ligands may complicate interpretation of the reaction between substrate complexes of the general acyl-CoA dehydrogenase and electron-transferring flavoprotein.

Mammalian acyl-CoA dehydrogenases catalyze the first step of β oxidation with the insertion of a trans double bond between C-2 and C-3 of their fatty acyl thioester substrates. Three classes of mammalian enzymes have been identified with overlapping substrate specificities for short (Green et al., 1954), medium (Crane et al., 1956; Hall & Kamin, 1975; Thorpe et al., 1979), and long acyl chains (Hauge, 1956; Hall et al., 1976). The enzyme with a broad specificity profile for me-

† From the Department of Chemistry, University of Delaware, Newark, Delaware 19711. *Received January 21, 1981.* This work was supported in part by a University of Delaware research foundation grant and a National Institutes of Health grant (GM 26643).

0006-2960/81/0420-4965$01.25/0